energies

Article

Performance Assessment of Solar Desiccant Air Conditioning System under Multiple Controlled Climatic Zones of Pakistan

Sibghat Ullah * and Muzaffar Ali

Mechanical Engineering Department, University of Engineering and Technology, Taxila 47050, Pakistan; muzaffar.ali@uettaxila.edu.pk
* Correspondence: sibghat.ullah@skt.umt.edu.pk

Abstract: Over the past decade, the integration of desiccant technology with evaporative cooling methods has proven to be highly effective and efficient in providing comfortable indoor environments. The performance of desiccant-based direct evaporative cooling (DEC) systems is strongly influenced by environmental conditions, and their output behavior varies across multiple climatic zones. It is not easy to assess the system performance in numerous climatic zones as it is a time-consuming process. The current study focuses on determining the feasibility of a solid desiccant integrated with a direct evaporative cooler (SDI-DEC) for three different climatic zones of Pakistan: Lahore (hot and humid), Islamabad (hot and semi-humid) and Karachi (moderate and humid). To serve this purpose, a specially designed controlled climate chamber with an integrated air handling unit (AHU) was installed to create multiple environmental conditions artificially. It could also provide global climatic conditions under temperature and absolute humidity ranges of 10 °C to 50 °C and 10 g/kg to 20 g/kg, respectively. The weather conditions of the selected cities were artificially generated in the climate chamber. Based on different operating conditions, such as inlet air temperature, humidity and regeneration temperature, the performance of the system was estimated using performance indicators like COP, dehumidification effectiveness, solar fraction and supply air conditions. Results showed that the maximum temperature achieved from solar collectors was about 70 °C from collectors with an area of 9.5 m^2. Moreover, the observations showed that when the regeneration temperature was increased from 60 °C to 80 °C, the COP of the system decreased about 41% in a moderate and humid climate, 28% in a hot and semi-humid environment and 23% in a hot and humid climate. The results revealed that an SDI-DEC system has the potential to overcome the humidity and cooling loads of the multiple climatic scenarios of Pakistan.

Keywords: desiccant; evaporative cooling; climatic zones

check for updates

Citation: Ullah, S.; Ali, M. Performance Assessment of Solar Desiccant Air Conditioning System under Multiple Controlled Climatic Zones of Pakistan. *Energies* **2023**, *16*, 6914. https://doi.org/10.3390/en16196914

Academic Editor: Vincenzo Costanzo

Received: 6 September 2023
Revised: 21 September 2023
Accepted: 23 September 2023
Published: 30 September 2023

1. Introduction

Energy consumption demand is increasing with rising living conditions. Environmental pollution and global heat are being raised along with greenhouse gas emissions [1]. Systems for heating, ventilation and air conditioning consume a huge portion of the overall energy used in building services. For instance, a survey by the International Energy Agency found that, in 2016, refrigeration systems accounted for 6% of all energy supplied to buildings [2]. In the last few decades, the energy demand for cooling systems has considerably increased due to population growth, technological advancements and materialistic living standards. Air cooling units account for almost 15% of the energy used worldwide. The conditions for a person's thermal comfort are considered in terms of the effective management of sensible and latent load. An air conditioning system should typically maintain indoor air temperatures of 18 to 26 °C and relative humidity levels of 40 to 70% in order to provide thermal comfort conditions to the occupants [3].

The performance of an air conditioner is determined in terms of the sensible heat ratio and its capacity to handle sensible and latent loads. The sensible heat ratio in conventional vapor-compression air conditioning systems is approximately 0.75 [4]. To remove the moisture from the air, it is cooled below its dew point temperature. Then, it is reheated to the appropriate supply temperature. This process of overcooling and reheating wastes a significant quantity of energy, which reduces the overall coefficient of performance (COP) of the system. Additionally, the condensation process in traditional air conditioning units fosters the development of germs and fungi and consumes a very large amount of electric energy. Hence, there is a need for some alternative cooling devices due to the high energy costs of these conventional systems and their ineffective management of latent load [5]. Renewable energy sources such as solar energy are one of the most attractive energy sources for air conditioning purposes due to their abundant availability. Different kinds of solar thermal collectors can be utilized to generate heat from solar radiation. Economic analysis has revealed that solar collectors have a great impact in terms of energy and operational costs as solar is an inexpensive source of energy [6,7].

For hot and humid regions in particular, solar-assisted desiccant cooling systems are an appealing and economical method for air conditioning applications. Due to the separate control of sensible and latent cooling loads, these systems are seen as a potential replacement for traditional air conditioning systems. In addition to this, the trend towards employing solar desiccant systems in buildings has increased due to the development of the technology and benefits such as the absence of chlorofluorocarbons, minimal electric power consumption, standard human comfort, energy savings and environmental protection [8]. Due to these features, desiccant systems can be used in supermarkets, the pharmaceutical industry, hospitals, the textile industry and other commercial buildings.

Desiccant systems are mainly divided into two main categories, solid desiccant systems and liquid desiccant systems. A liquid desiccant system has two components, the regenerator and the absorber, and it requires lower heat for regeneration as compared to a solid desiccant system. Corrosion and initial capital cost are the main drawbacks of liquid desiccant systems [9]. A solid desiccant system is used to dehumidify humid air by means of the difference in the partial pressure of the humid air and the surface of the desiccant wheel. Different kinds of desiccant materials are used to dehumidify the humid air. Desiccant wheels can be either fixed-type or rotary-type [10]. A rotary-type desiccant system is commonly used for air conditioning applications due to its easy handling and requiring less maintenance of the wheel. Zeolite, silica gel and hybrid materials, sometimes sieve-type, are most often used as desiccant materials in desiccant systems [11]. Pressure drops in solid desiccant systems negatively impact the performance of the system. Moreover, the critical issues associated with solid desiccant air conditioning systems are the size, compatibility, competitive design and requirement of high regeneration temperatures. Mostly, solid desiccant systems preferably need a lower temperature regenerated desiccant material to save energy. Solid desiccants have less ability to filter out microorganisms as compared to liquid desiccant systems [12].

The literature on desiccant air conditioning systems includes extensive research because of the significance of such cooling systems. Most of the studies have concentrated on the modelling and simulation of the desiccant wheel, which is the key component of any desiccant cooling system [13,14]. Numerous studies on advanced desiccant materials concentrate on the thermal and adsorption features of the desiccants to assess the impact of their physical and chemical properties [15]. Nilofar et al. [16] studied the properties of desiccant materials and concluded that environmental conditions and cost are the main factors in selecting the desiccant material. Among different desiccant materials, it was mentioned that carbon-based composite materials show promising advantages in desiccant cooling systems. Chen et al. [17] presented the idea of hybrid materials and highlighted results showing that hybrid materials have 41% more moisture removal capacity than silica gel. Reza et al. [18] depicted how different kinds of solar collectors are used to convert sunlight into useful energy that can be utilized in desiccant systems. The author concluded that collectors that operated at low temperatures were the most efficient and cost saver. Ali et al. [19] developed a numerical model using Dymola software to examine five different configurations of desiccant cooling systems under five different climate zones to represent the worldwide metrological data. The authors remarked that the ventilated Dunkle cycle suits Sao Paulo, Vienna and Adelaide the best. Rafique et al. [20] investigated the coefficient of performance (COP) of desiccant cooling systems in different cities of Saudi Arabia and reported that the achieved COP was in the range of 0.275 to 0.476. Jani et al. [21] use TRNSYS simulation via considering a hybrid desiccant system under a 1.8 kW load of cooling and found that at the exit of the desiccant wheel, air humidity decreases significantly. Gao et al. [22] conducted numerical studies on a desiccant system integrated with a cross-flow indirect evaporative cooler using the heat transfer units (HTUs) method under different ranges of parameters and concluded that the inlet temperature and humidity of the air should be less than 35 °C and 18 g/kg for the best results. Fong et al. [23] studied the simulation of the year-round application of solar-assisted desiccant through considering six various configurations and showed that 35.2% of energy can be saved. In another study, Ali et al. [24] evaluated the different cycles of desiccant cooling systems, such as recirculation, Dunkel and ventilation in different climate zones. Ventilation and recirculation cycles are mostly used for desiccant air conditioning applications. Belguith et al. [25] presented the model study on different modes of desiccant cooling systems like recirculation, Dunkle and ventilation cycles. COPs of ventilation recirculation and Dunkle modes are 1.89, 1.13 and 1.71, respectively. The COP results showed that ventilation mode efficiency was better than the other modes [26].

Since the middle of the 20th century, desiccant evaporative cycles have been patented and refined. They are thermally driven air conditioning processes that typically combine adsorptive dehumidification and evaporative cooling. Desiccant-based evaporative cooling systems are thought to be one of the best alternatives to the vapor-compression system in humid and hot climates. Integrated evaporative cooling with a solid desiccant unit has received much attention in an effort to expand the application of evaporative cooling [27]. Khalid et al. [28] studied the DEC system for a two-story building in Baghdad. They concluded that the COP of the evaporative system increased by 41.3% to 47.7% when cooler efficiency was enhanced from 0.1 to 0.9. Hindoliya et al. [29] collected the hourly data of ambient conditions for 60 big cities in India to check the potential of the DEC system. It was observed that the northwestern and central regions of India have huge potential for the utilization of the DEC system, whereas the northern, coastal and eastern parts show less potential. Bourdoukan et al. [30] performed an experimental analysis of a solar-powered desiccant air handling unit; results highlight that the COP of the system is 0.4 on a moderate and humid day. Moreover, the efficiency of vacuum tube collectors is 0.55. Heidarinejad et al. [31] used the numerical technique to calculate the desiccant air conditioning application for the multi-climate of Iran. They concluded that in areas where the humidity level is high, the desiccant system with a DEC system is suitable for cooling purposes. Similarly, Delfani et al. [32] considered three modes of the desiccant system for three climatic zones, represented by the cities Babol, Abadan and Bushehr, via TRNSYS simulation and remarked that the COP of the system decreased from 1.28 to 0.6 when the regeneration temperature was increased from 100 °C to 120 °C. Parmar et al. [33] presented a numerical analysis of the performance of the desiccant system for the three-climate condition of India. They concluded that the desiccant system is suitable for the warm and humid climate of India. Numerical and simulation-based research studies on desiccant air conditioning systems are briefly described in Table 1.

Table 1. Summary table for previous overview papers.

Author	Year	Methodology			Findings
		Experimental	Simulation	Opt.	
Ghaddar et al. [34]	2021		✓	✓	The use of PCM in desiccant cooling can reduce 87% of energy, and the Trombe wall saves 55% of energy compared with the auxiliary heater.

Table 1. *Cont.*

Author	Year	Methodology			Findings
		Experimental	Simulation	Opt.	
Khosravi et al. [35]	2020	✓			A comparison study of different desiccant materials concluded that desiccant-assisted evaporative cooling systems have 17 to 62% higher cooling capacity compared to standalone direct evaporative cooling systems.
Lee et al. [36]	2020		✓		The simulation of a desiccant system with three modes, direct evaporative cooling (DEC), indirect evaporative cooling (IDEC) and a hybrid system, was studied and it was found that the DEC system has the lowest COP. In contrast, IDEC has maximum COP when the outdoor temperature is below 40 °C, but beyond this temperature, the hybrid system has the maximum COP.
Song et al. [37]	2020		✓		Simulation study conducted on photothermal (PV) for regeneration, phase change material (PCM) for night storage of energy and Maisotsenko cycle (M-Cycle) for cooling. It was found that the maximum total COP achieved was 0.404. PCM contributed to the improvement of thermal efficiency.
Farooq et al. [38]	2020		✓	✓	TRNSYS simulation was carried out for the city of Lahore under three configurations (C1, C2, C3). For C1, an auxiliary heater is installed in the air conditioning cycle. In C2, an auxiliary heater is installed in the solar loop, and in C3, there is no evaporative cooler; only a vapor compression system is used for cooling, and an auxiliary heater is installed in the cooling loop. A comparison of all these configurations concluded that C1 shows the best performance.
Berardi et al. [39]	2020		✓		Simulation work performed by the author using TRNSYS 17 software. The ground source heat exchanger is used as post-cooling after the desiccant wheel. Results show that the best COP was achieved when solar fraction (SF) was 63.6% and payback cost after 6.8 years.
Delfani et al. [32]	2020		✓		Numerical investigation carried out in TRNSYS simulation software using M-Cycle with desiccant system in three different configurations for different cities. It was found that COP was reduced by 53% when the regeneration temperature increased from 100 °C to 120 °C.
Ahmad et al. [40]	2020		✓		TRNSYS simulation software was used for the three different configurations and a comparison study was carried out with already-published data.
Karami et al. [41]	2019		✓		Transient simulation of the desiccant system. Three different mixtures of return air are considered. The heat wheel efficiency enhances COP.

Table 1. *Cont.*

Author	Year	Methodology			Findings
		Experimental	Simulation	Opt.	
Ali et al. [24]	2015		✓		Performance analysis of 5 DEC configurations in 5 different climate zones. Three standard cycles and two modified configurations are used. The ventilation cycle suits the climate of Pakistan.
Heidarinejad et al. [31]	2011		✓		Checked the performance of the hybrid desiccant system for the climate of Iran and concluded after considering different outdoor conditions that the hybrid desiccant system is suitable for humid climates.
Parmar et al. [33]	2011		✓		Presented the numerical technique for three cities in India and concluded that a desiccant air conditioning system is best for warm and humid climates.

It can be concluded from published studies that a lot of simulation-based research studies cover the performance of desiccant air conditioning systems and found limited experimental research work in specific climatic zones. However, no study covers the experimental analysis of the SDI-DEC under artificially generated climate conditions for different global climatic zones. Therefore, in the current study, the SDI-DEC is integrated with an artificially developed controlled climate chamber, and the performance is investigated under the controlled environmental conditions of three cities of Pakistan: Karachi (moderate–humid), Islamabad (hot–semi-humid) and Lahore (hot–humid). These climatic conditions were artificially created within a specially designed climate chamber through AHU. The performance of the SDI-DEC is evaluated against each climate zone in terms of supply temperature, supply humidity, dehumidification effectiveness and coefficient of performance (COP). Moreover, the performance of solar evacuated tube collectors is also assessed based on varying the area of the collectors from 9.5 m^2 to 4.8 m^2.

A control room is installed to create the multiple climatic zones of these cities, and a test room is used to validate the SDI-DEC system's performance against the selected climate scenarios. The performance of the SDI-DEC is assessed in terms of the COP of the system, dehumidification effectiveness, solar fraction and different supply air conditions. To evaluate the effects of outdoor weather conditions on the performance of the SDI-DEC, it is experimentally investigated for different outdoor dry bulb temperatures and humidity. To compare the investigated desiccant systems with a direct evaporative cooler (DEC), the potential of a DEC to achieve thermal comfort based on outdoor controlled design conditions for three selected cities was analyzed.

2. Materials and Methods

The performance of the solar desiccant integrated direct evaporative cooler (SDI-DEC) is highly dependent on the outdoor environmental conditions. The SDI-DEC is installed to ensure the desired thermal comfort. It is to be evaluated in different climatic conditions for selected cities in Pakistan, Karachi (moderate–humid), Islamabad (hot–semi humid) and Lahore (hot–humid), to make it a feasible solution for each location. Figure 1 shows the map of the selected cities of Pakistan. The present study is to investigate the SDI-DEC system's performance in multiple climatic conditions of Pakistan under controlled environmental conditions. Weather data and design conditions of Pakistan have been obtained from the Weather Atlas data website and are shown in Figure 2 [42]. Environmental climate conditions for Lahore, Karachi and Islamabad are considered and created in the control room according to the design conditions provided in Table 2.

Table 2. Climate zones of selected cities of Pakistan.

City	Climate Condition	May		June		July		Longitude (°E)	Latitude (°N)
		Avg Temperature (°C)	Avg Absolute Humidity (g/kg)	Avg Temperature (°C)	Avg Absolute Humidity (g/kg)	Avg Temperature (°C)	Avg Absolute Humidity (g/kg)		
Karachi	Moderate–Humid	34	16.3	35.6	17.9	35.5	20.3	67.01	24.86
Lahore	Hot–Humid	33.9	13.6	37.3	15.8	39.5	17.3	74.35	31.56
Islamabad	Hot–Semi Humid	30.5	12.3	35.7	14.5	38.7	16.2	73.04	33.72

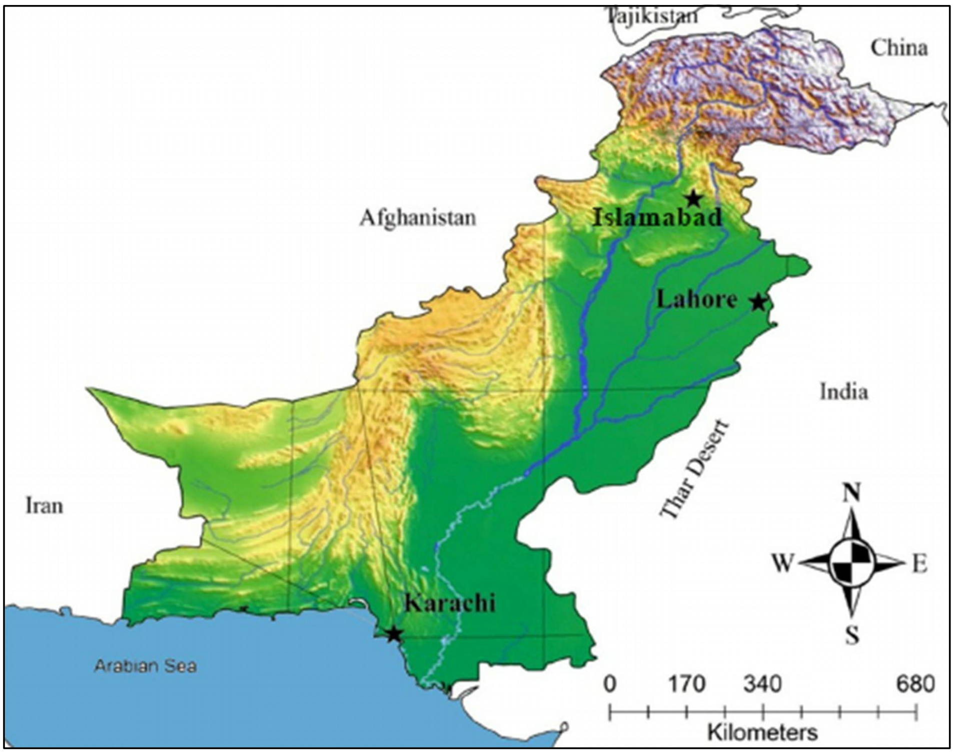

Figure 1. Geographical location of selected climate zones of Pakistan.

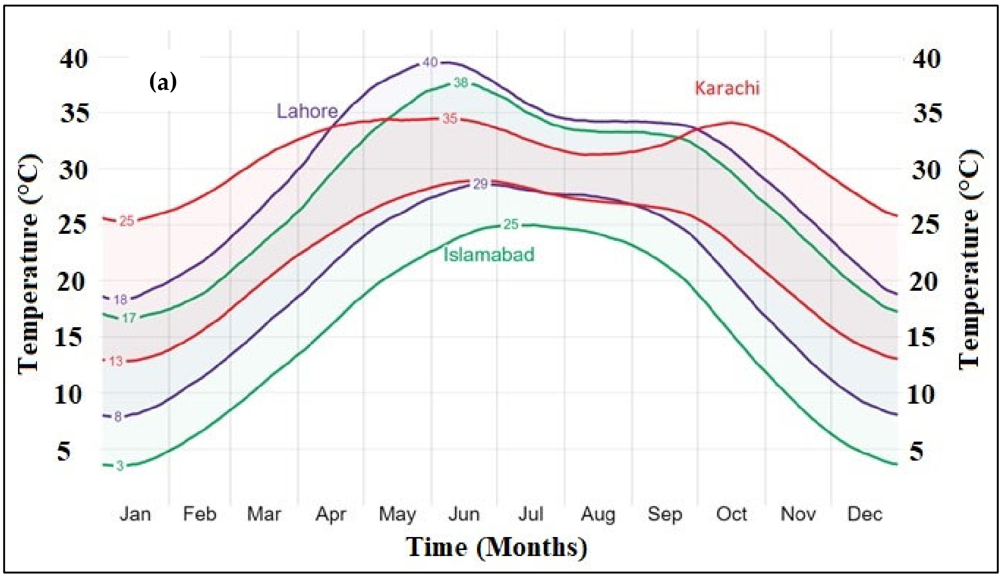

Figure 2. *Cont.*

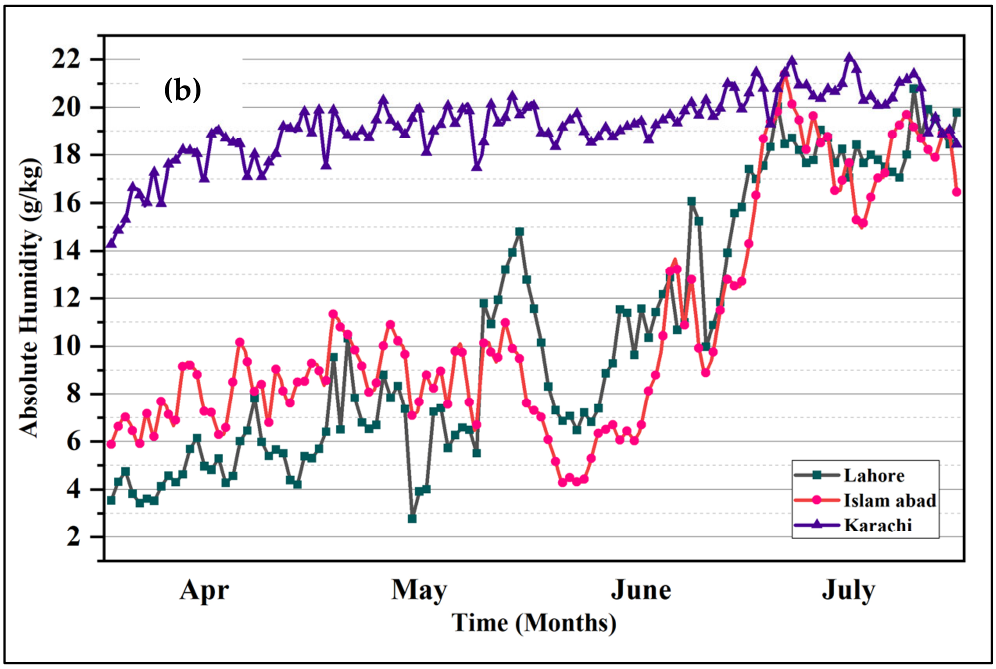

Figure 2. Climate conditions of selected cities of Pakistan: (**a**) dry-bulb temperature, (**b**) absolute humidity.

To evaluate the SDI-DEC system for different climatic conditions, the climate chamber or control room is used to artificially produce weather conditions of various locations using the air handling unit (AHU) that is integrated within the control room. The AHU includes a compressor, heater and humidifier. The purpose of the compressor is to produce wintry conditions or provide cooling in the control room, whereas the heater provides heated air and creates hot-weather conditions in the control room. The humidifier intends to add moisture content to the air. It, therefore, helps to provide the desired humidity levels as per the required weather conditions upon which the system is to be evaluated. The controller is used to operate the AHU and to set the desired temperature and humidity levels in the control chamber. The SDI-DEC system is effectively tested under a variety of controlled weather conditions for a predetermined amount of time. Input design conditions consist of the supply air temperature and humidity, as these two are the most important parameters and can affect the thermal comfort level of humans. The feasibility of the SDI-DEC system for the mentioned cities has been evaluated. An extensive experimental study was designed and performed to test the installed system at a range of input ambient conditions. The selected domain ranges between 30 and 40 °C dry bulb temperature, and the absolute humidity ratio ranges from 12 g/kg to 20 g/kg, covering various outdoor conditions for the multi-climate cities of Lahore, Karachi and Islamabad. Data acquisition was performed with multiple sensors to note the readings of temperature and humidity, which were located at all inlet and outlet points for each component of the installed system. Through examining the data obtained from the acquisition system, different input parameters which have the potential to affect the system output performance were considered.

3. System Description

The solar-assisted desiccant-based evaporative cooler (Sol-DEC) mainly consists of three parts for testing purposes: (i) solar evacuated tube collectors (SETCs) for the heating of water, (ii) a rotary desiccant wheel integrated with a direct evaporative cooler, (iii) a control room to maintain the temperature and humidity artificially at an inlet of the desiccant wheel (DW), and a test room to check the performance of the system. A schematic diagram of the whole system with exact sensor locations is shown in Figure 3.

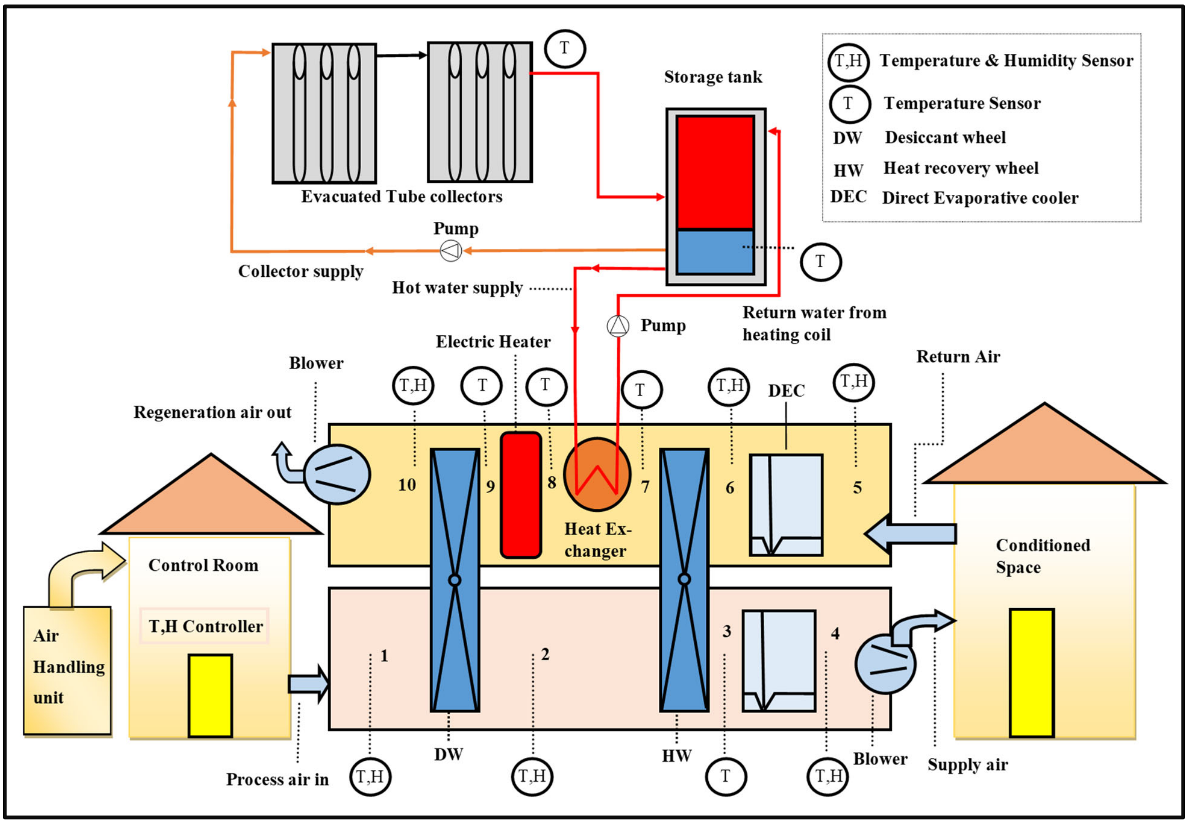

Figure 3. Schematic diagram of a solar desiccant integrated direct evaporative cooler (SDI-DEC).

3.1. Solar Evacuated Tube Collectors

Solar evacuated tube collectors (SETCs) are installed on the roof of the Department of Energy Engineering, University of Engineering and Technology, Taxila, Pakistan, to harvest the energy of the sun to heat the water at a desired level. SETCs, along with the storage tank, are shown in Figure 4. Since DW is a thermally driven cycle, heat energy input is necessary to regenerate the desiccant material of the DW. Different conventional methods, such as waste heat, gas burners or electric heaters, can provide this thermal energy. However, in this research, hot water is used as the working fluid and SETCs are used to capture solar energy from the sun. SETCs are used as these collectors have less thermal loss as compared to flat plate solar collectors. A storage tank with a capacity of 0.3 m^3 was installed to store the hot water. Rock wool is used to insulate the storage tank of water. Hot water circulates between the SETCs and storage tank with the help of a small magnetic-type water pump; a magnetic water pump delivers the water at the flow rate of 560 kg/h. Ball valves are installed at different locations to control water flow in the closed cycle of the SETCs. Glycol is used in a closed process between the SETCs and the storage tank to avoid steam production in the pipes due to high radiation. Steam in pipes can slow down or stop the circulation of the water. For safety purposes, a steam relief valve is installed within the storage tank to release steam if it is generated. Two K-type thermocouple water temperature sensors are installed at the bottom and top of the storage tank. One thermocouple water temperature sensor was installed on the outlet pipe from the SETCs. The temperature gradient required to maintain water circulation between the SETCs and the storage tank was 8 °C. An electric water heater is installed in the storage tank as a backup to achieve the desired temperature if solar heat is not available. A separate solar controller is installed to control the on/off switch of the magnetic pump and the electric water heater of the storage tank. The solar controller can set the temperature of the electric water heater up to 80 °C; the maximum temperature drop recorded in the air-to-water heat exchanger was 4 °C. To regenerate the desiccant wheel, hot water was supplied from the storage tank to the air-to-water heat exchanger through gravity. However, a separate water pump was used to pump the water from the air-to-water heat exchanger to the storage tank to continue the water cycle.

Figure 4. Solar evacuated tube collectors with hot water storage tank.

3.2. Solar Desiccant Integrated Direct Evaporative Cooler

The physical setup of the system is shown in Figure 5. The whole system consists of solar evacuated tube collectors; a honeycomb structure comprising a rotary desiccant wheel (DW), heat recovery wheel (HRW), direct evaporative coolers (DECs), electric heater, and fin-type air-to-water heat exchanger; suction fans; a control room (chamber 1) and a test room (chamber 2). The DW is the heart of the system to control the latent load. The integration of the DEC is useful to handle the sensible load. The system is mainly divided into two domains of air. One is the process side of the air, and the second is the regeneration side of the air. Heat and moisture come from the control room and enter the system through the duct at point 1 as the process air side using a suction fan. Humid air passes through the DW at point 1 and gets dehumidified after passing through from the DW as it is made of silica gel and can control the moisture of the air. Silica gel is used as a desiccant material and has a natural affinity to absorb moisture due to the difference in vapor pressure of water vapors. After the dehumidification of the air, the air reaches a high temperature because the absorption process air gets saturated at the process side of point 2. This hot air is needed to cool down. For this purpose, an HRW is installed before the DEC. The honeycomb structure of the HRW is made of aluminum and acts as a rotary air-to-air heat exchanger. Cool air comes from DEC 2, which is placed at the regeneration side. At point 3 of the process side, the air temperature drops due to the HRW. After that, the DEC is installed to control the sensible load at point 4 of the process side. The DEC is used to cool down the process air to achieve thermal comfort. In this process, air is sucked through the suction fan and supplied into the test room to check the system performance. On the other side, regeneration air is mainly used to make DW reactive for continued operation. After some time, DW gets saturated and needs hot air to remove the absorbed moisture. To fulfil the DW's requirement for hot air, SETCs are used. Furthermore, the electric heater is also used as an auxiliary heater. So, to complete this whole cycle, air enters into the regeneration side at point 5 through the second suction fan. The second DEC is installed at the regeneration side to supply cool air to the HRW at point 6. Due to air-to-air heat exchange, the temperature of air increases at point 7. After that, the air-to-water heat exchanger is installed to raise the temperature of the regeneration air. Hot water comes from the SETCs and circulates through the fin-type air-to-water heat exchanger. Regeneration air gets hot after passing through the fin-type air to the water heat exchanger at point 8. An electric heater is installed after the air-to-water heat exchanger to maintain the temperature of the regeneration air at point 9. At last, this hot regeneration air passes through the desiccant wheel at the regeneration side of the desiccant wheel to remove the moisture contained by the DW and to reactivate the DW at point 10. Separate humidity and temperature sensors are used to check each component's performance in different locations of the whole test rig, as shown in Figure 3. Specifications of all the components installed in the SDI-DEC are shown in Table 3.

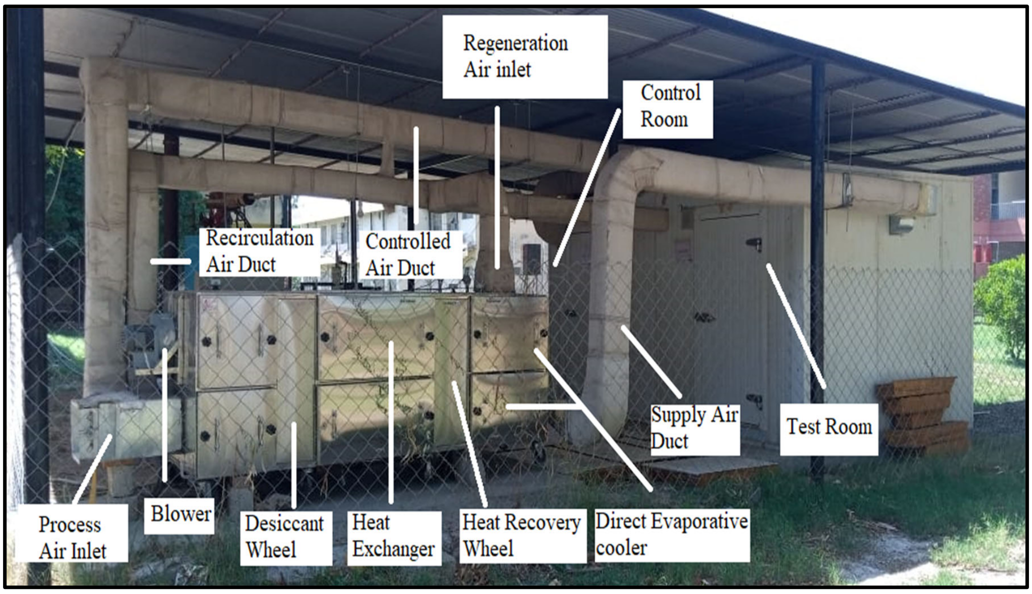

Figure 5. Experimental setup of SDI-DEC.

Table 3. Specifications of components used in SDI-DEC.

Solar evacuated tube collector		**Desiccant wheel with cassette**	
Model number	JMC-5818	Model no.	KM-0058
Pipe material	Glass	Type	Rotary type
Vacuum tube material	Borosilicate glass 3.3	Dehumidification capacity	19 kg/h
Heat pipe	Red Copper	Absorbent material	Silica Gel
Manifold casing	Aluminium alloy	Size	700 × 200 mm^2
Insulation layer	Rock Wool	Capacity	1500–2000 CFM
Vacuum tubes	40	Moisture removing capacity	Inlet up to 22 g/kg
Working pressure	6 bars		Outlet 10–12 g/kg
Heat recovery wheel with cassette		**Blowers**	
Brand name	Holtop	Type	Centrifugal Fan
Type	Rotary type	Blade material	Aluminum
Size	700 × 200 mm^2	Inlet diameter	183 mm
Capacity	1500–2000 CFM	Air capacity	3900~4600 m^3/h
Enthalpy	65–80%	**Variable electric heater**	
Temperature	70–85%	Power	0.5–15 kW
Fin thickness	0.12 mm	Temperature range	60–120 °C
Materials	Aluminum & 3A molecular sieve	Material	Stainless steel
Liquid flow rate	1–5.5 m/s	-	-
Air-to-water heat exchanger			
Working fluid	Water-glycol	Heat transfer rate	10–30 kW
Water flow rate	100 LPM	Maximum temperature	120–150 °C
Type	Fin type and Cross-flow	-	-
Air handling unit			
Temperature range	10–50 °C	Load Capacity	2.5 ton
Relative humidity	95%		

3.3. Control Condition Scenario

The SDI-DEC is tested under control conditions; for this purpose, an insulated room setup is installed on the ground near the Department of Energy Engineering, University of Engineering and Technology Taxila. This insulated room was first designed carefully in 3D view and then installed. The total dimensions of the installed room setup are 4.57 × 3.05 × 3.05 m^3, and it is separated into two rooms: the test room and the control room/climatic chamber. The control room creates an artificial environment condition to supply the desired inputs in terms of temperature and humidity to the SDI-DEC. The test room is used to check the SDI-DEC system's performance under load conditions. An air handling unit (AHU) is installed in the control room to create artificial conditions in the control room. Artificial conditions are made in terms of cooling, heating and humidification. The AHU consists of three parts: (i) a vapor-compression system for cooling, (ii) a humidifier for humidification of the air and (iii) an electric heater to maintain the heating needed in the control room. Maintaining a wide range of testing conditions can create all forms of weather, like dry or humid, hot or cold, in the control room. Figure 6 shows the real-time installation of both rooms. The dimensions of the control room and test room are given in Table 4. To control supply conditions, air from the control room moves to the test rig as the input of the DW through duct 1 (controlled air duct). Proper insulation of duct 1, which is made of sheet metal, is maintained to reduce energy losses. Duct 2 (supply air duct) is used to supply the process air from the SDI-DEC to the test room. Duct 3 (load duct) connects the control room and tests from the top of both rooms. Duct 3 is used to create load conditions in the test room to check the SDI-DEC's performance against different loads. This ducting system is made of sheet metal and properly insulated to reduce the heat loss from the ducts. A schematic diagram of ducting within the SDI-DEC is shown in Figure 7. Different volume control dampers (VCDs) of rectangular shapes are installed at various suitable locations to control the air flow rate in all of the ducts.

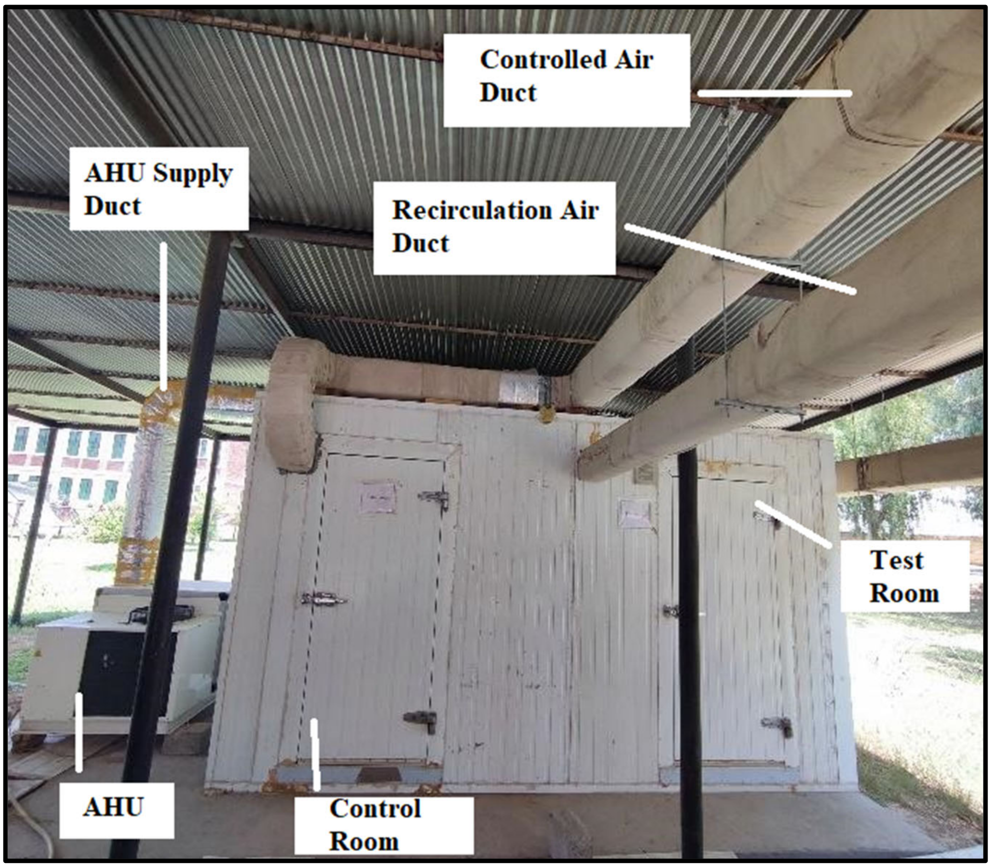

Figure 6. Chamber of control and test rooms.

Table 4. Dimensions of the complete test room.

Chamber-1		Chamber-2	
Length	1.42 m	Length	3.05 m
Width	3.05 m	Width	3.05 m
Thickness	0.051 m	Thickness	0.051 m

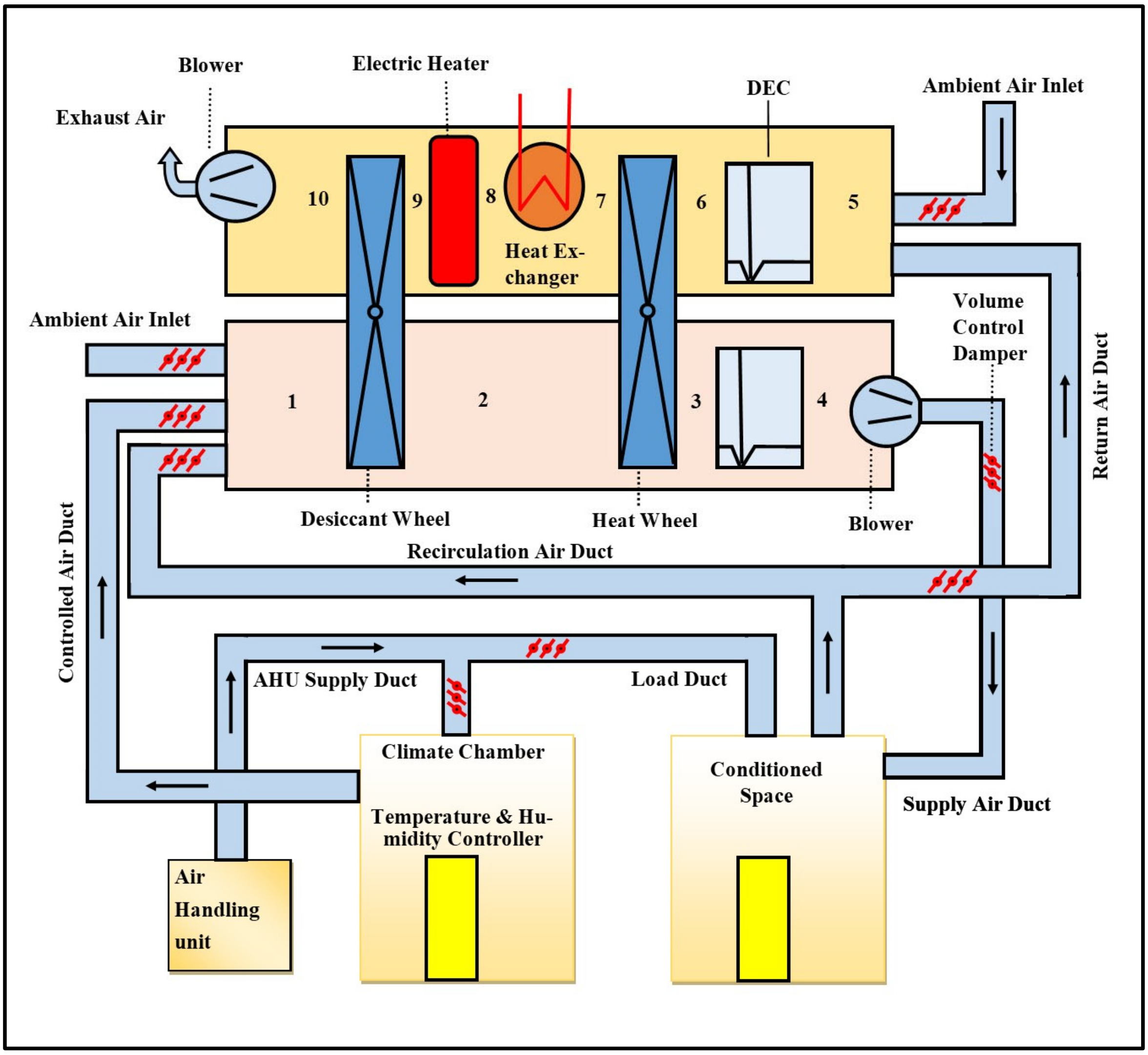

Figure 7. Schematic diagram of ducting.

3.4. Measurement and Controlling Setup

Experiments are carried out under a proper controlling and monitoring setup. The temperature, relative humidity, electric current and rotation of both air suction fans are measured in the test rig. Different humidity and temperature sensors are used separately at various locations of the test rig. The electric signals of temperature sensors are recorded using transmitters and monitored through a computer-controlled data acquisition system. Three variable frequency drives (VFDs) are installed in the control panel; two of them are used to control the speed of two fans, and one is used to control the speed of the desiccant wheel. The SDI-DEC system has four types of controls: (i) a programmable logic controller (PLC), (ii) an electric heater controller, (iii) a solar system controller, and (iv) a controller for the AHU. The function of the PLC is to (i) control the operation of the test rig; (ii) control the on/off operation of the DW, HRW, fans, electric heater and water pumps; (iii) regulate the speed of both fans and the DW; and (iv) control the magnetic contractors through relays. All the installed sensors give input to the PLC. After PLC decoding, this input is displayed as reading on the human–machine interface (HMI) screen. The HMI is used to monitor the values of all the sensors that were installed in the test rig and is also used to set the desired value for the type of electric heater and rpm of fans. Electric controllers control the electric fin-type heater to maintain the regeneration operation and protect the electric fin-type heater from any fluctuation in electric current. The solar system controller is installed separately to switch on/off both the magnetic pump installed between SETCs and the hot water storage tank as well as the auxiliary heater installed in the hot storage tank. The controller records the readings of the K-type thermocouples installed in the hot water storage tank and SETCs. The AHU controller is installed in the control room to operate the AHU. The vapor-compression system, fan, electric heater and humidifier installed in the AHU are run through this controller. The AHU controller is also used to set the desired heating, cooling and humidification value in the control room. Figure 8 shows the controller setup used to control the whole test rig in the control environment. Solar radiation is measured through the pyranometer with an accuracy of 1 W/m^2. Specifications of all the temperature and humidity sensors and other instruments used in the testing are given in Table 5.

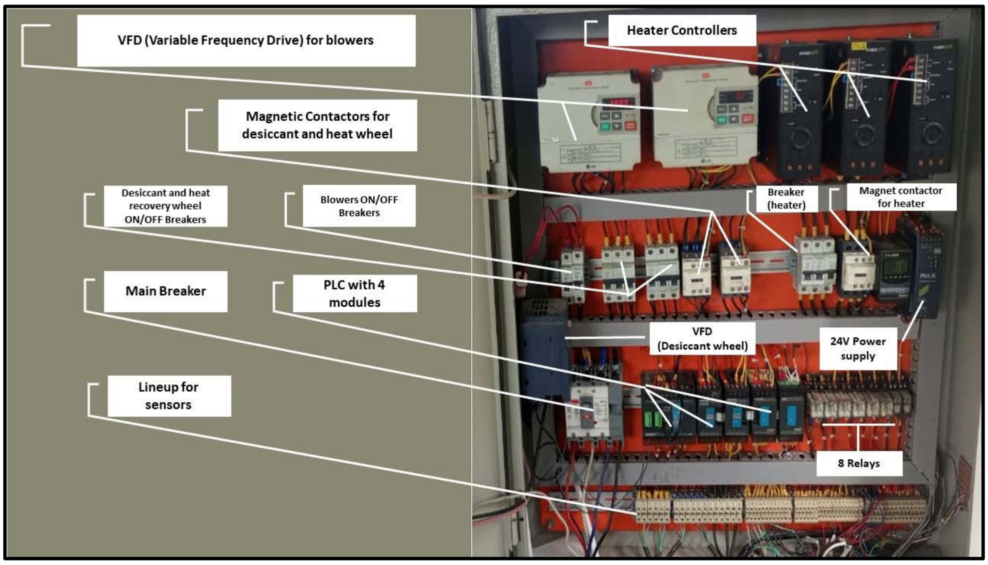

Figure 8. Control panel installation setup.

Table 5. Specification of measuring instruments.

Measurement	Measuring Instrument	Measuring Range	Accuracy
Temperature	Pt-100	−10–100 °C	±0.15 °C
Relative humidity	PHT 3109	0–99%	±2%
Air flow rate	Anemometer	0.1–20 m/s	±0.01 m/s
Solar radiation	Pyranometer	0–1500 W/m^2	1 W/m^2
Water temperature	K-type Thermocouple	0–200 °C	0.3%
Water flow rate	Flow transducers	0.1–120 LPM	0.5 LPM

3.5. Data Reduction

The performance of individual components and the integrated system configuration are evaluated and highlighted using various performance indices. These indices are calculated based on experimental data obtained during testing and analysis.

The heat energy gain from the SETC is calculated as:

$$Q_{gain} = \dot{m}c_p(T_{c,out} - T_{c,in}) \tag{1}$$

The solar fraction is calculated as follows:

$$SF = \frac{Q_{gain}}{Q_{gain} + Q_{sol}} \tag{2}$$

The dehumidification effectiveness of the system is defined as the actual reduction in the specific humidity of the air relative to the maximum possible reduction in the humidity ratio. It is given as follows.

$$E_d = \frac{\omega_1 - \omega_2}{\omega_1} \tag{3}$$

The COP of the system is calculated from the following relation:

$$COP = \frac{h_1 - h_4}{h_9 - h_7} \tag{4}$$

4. Results and Discussion

4.1. Solar Water Heating System

The solid desiccant cooling system utilizes solar energy to cope with latent load via heating water through solar thermal collectors. Solar energy is required to regenerate the desiccant wheel during the regeneration process; SETCs are used to serve this purpose. Solar thermal energy varies with respect to time due to the fluctuation of solar intensity throughout the day. Figures 9 and 10 depict the variation in the collectors' temperature along with solar irradiance for two different collector areas of 9.7 m^2 and 4.8 $m^{2,}$ respectively. It can be observed that solar radiation significantly influences the outlet temperature of the water from the collectors. In the morning, solar irradiance is low, which results in low water outlet temperature. Similarly, in the evening, the outlet temperature drops due to the low intensity of solar radiation. The collector's size strongly influences the efficiency of a solar thermal collector; a larger area results in higher outlet temperatures, ultimately improving the overall performance of the solid desiccant cooling system. The maximum outlet temperature achieved from collectors with an area of 9.7 m^2 was 69.1 °C, and 60 °C from collectors with an area of 4.8 m^2.

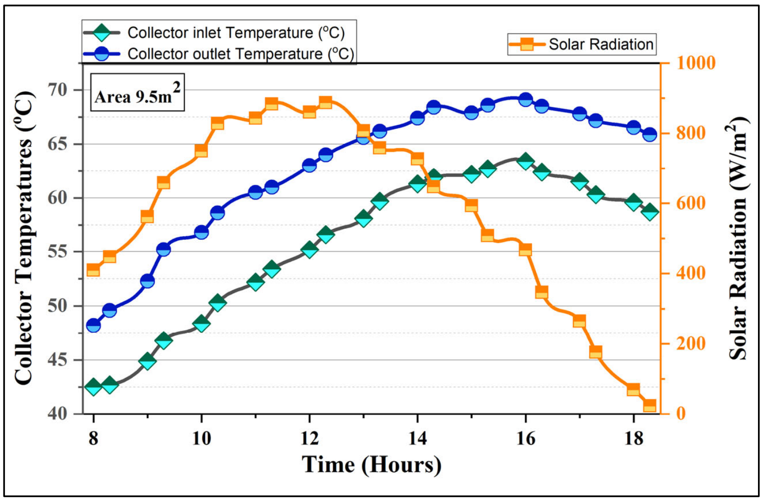

Figure 9. Variation of collector's temperature with solar irradiance for collector area of 9.5 m^2.

Figure 11 represents the variation in solar fraction for different collector areas with respect to time throughout the day. The observations show that the solar fraction is high when the collector area is 9.5 m^2 (configuration 1). The fact is that the larger collector area provides a large surface area for the absorption of solar radiation, which results in a high potential for energy harvesting, leading to an increase in solar fraction. In addition to this, solar intensity also influences the solar fraction. During peak sunshine, the intensity of solar radiation is high. Hence, more energy is present at collectors to convert, increasing the solar fraction. It can be observed that for configuration 1, the maximum solar fraction achieved was about 71%, whereas for configuration 2, the maximum solar fraction achieved was 49%.

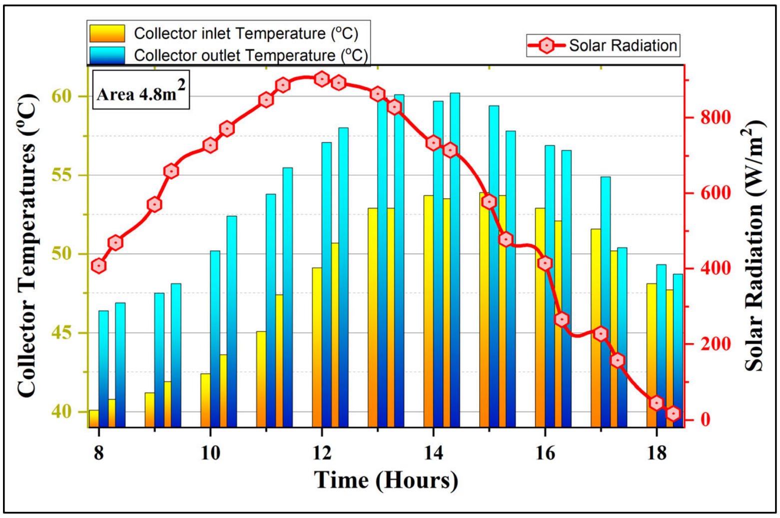

Figure 10. Variation in temperature of collector loop for area of 4.8 m^2.

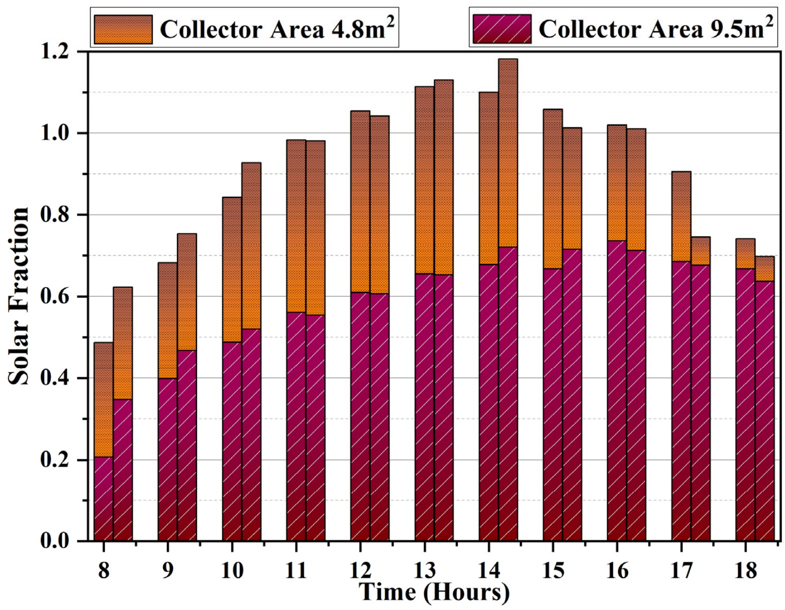

Figure 11. Variation in solar fraction for two configurations.

4.2. Solid Desiccant Integrated Direct Evaporative Cooler

Figure 12 depicts the performance of the system in terms of outlet air temperature and outlet air humidity for the hot and humid climate of Lahore at three different regeneration temperatures. It can be observed that T_{pin} and ω_{pin} increase from May to July. The average process inlet temperature in May, June and July is 33.9 °C, 37.3 °C and 39.53 °C, whereas the average inlet humidity ratio in these months is 13.6, 15.86 and 17.32 g/kg, respectively. The process inlet conditions, including the inlet humidity and inlet air temperature, have a significant impact on the performance of the desiccant air conditioning system. The process outlet humidity rises when the process inlet humidity is increased from May to July. This is because when the inlet air becomes more humid, the desiccant wheel can absorb more moisture from the process air, and it becomes saturated after some time. As a result, the desiccant wheel did not remove the moisture from incoming air at the desired levels. Hence, supply air humidity increases. In addition to this, when this process air is further passed through the DEC, it also increases the humidity level and reduces the temperature in the conditioned space.

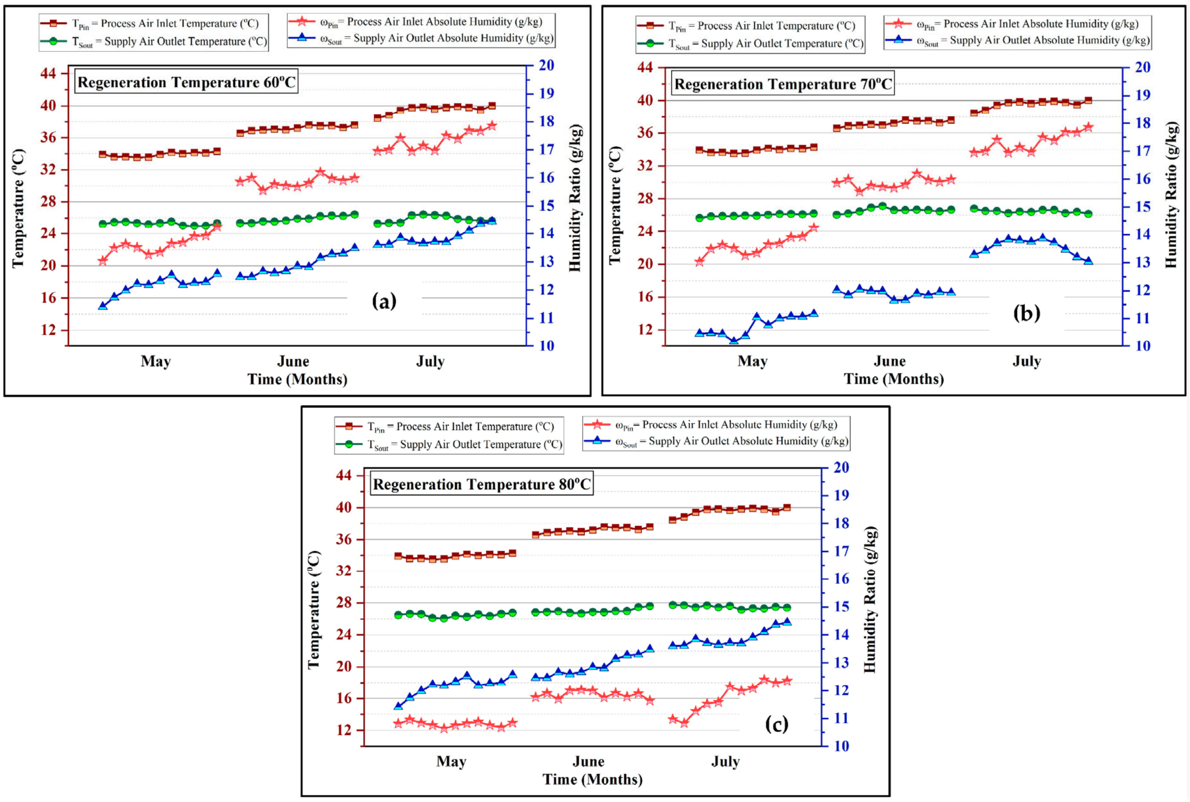

Figure 12. Lahore: variation in temperature and humidity; (**a**) T_{reg} = 60 °C, (**b**) T_{reg} = 70 °C, (**c**) T_{reg} = 80 °C.

Moreover, the observations show that the supply air temperature increases with an increase in inlet air temperature from May to July. The reason behind this is that due to the rise in temperature at the exit of the desiccant wheel on the process side, the process inlet temperature or regeneration air temperature increases. Furthermore, the regeneration temperature also significantly impacts the supply air humidity and supply air temperature. As the regeneration temperature increases, the capability of the desiccant wheel to remove moisture from process air increases. Hence, it results in lower outlet humidity at higher regeneration temperatures.

In the climate conditions of Islamabad, where temperatures and specific humidity levels vary across the months, the system's performance will be influenced accordingly, as illustrated in Figure 13. The average temperature in Islamabad in May, June and July is 30.5 °C, 37.7 °C and 38.7 °C, respectively. The increase in average specific humidity from May to July implies higher moisture content in the process air. It was found that the outlet air humidity decreases when the regeneration temperature is increased from 60 °C to 70 °C. The reason is the increased moisture removal capability of the desiccant wheel at higher regeneration temperatures. The maximum outlet humidity for this hot and semi-humid climate at T_{reg} of 60 °C, 70 °C and 80 °C is 13.5, 12.3 and 11.9 g/kg, respectively.

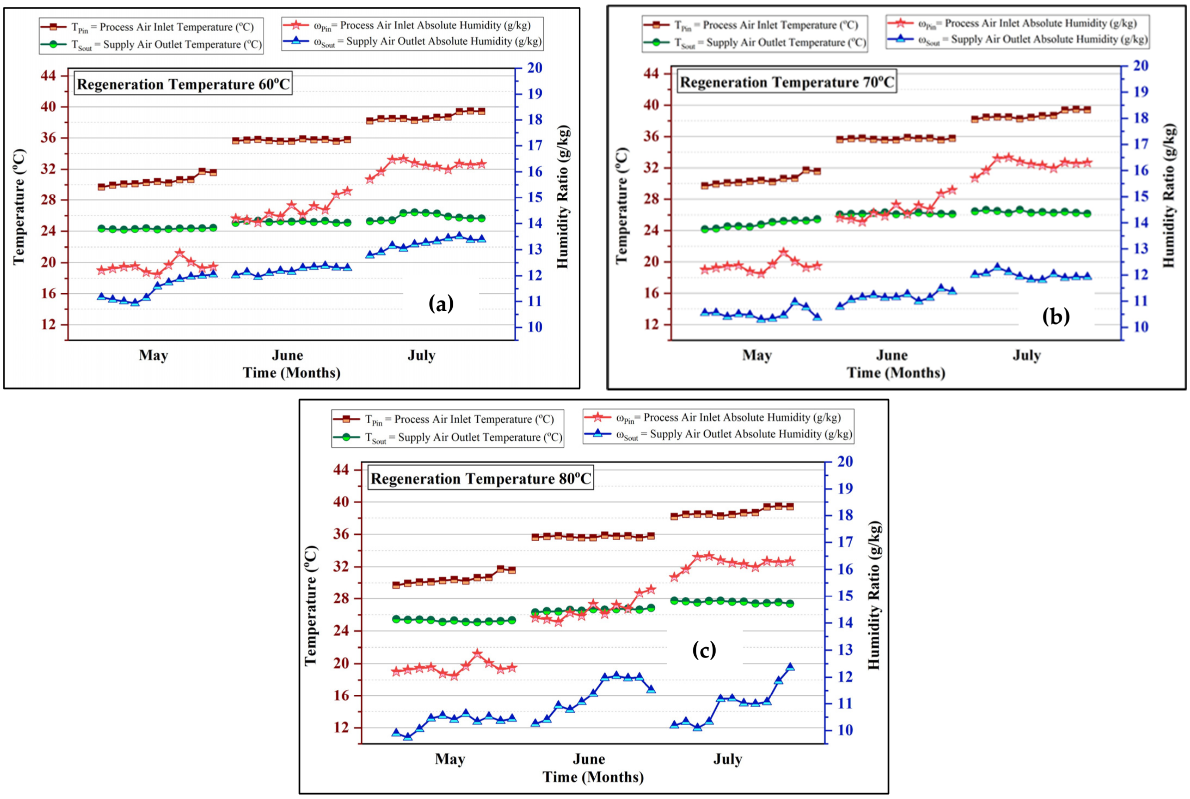

Figure 13. Islamabad: variation in temperature and humidity; (**a**) T_{reg} = 60 °C, (**b**) T_{reg} = 70 °C, (**c**) T_{reg} = 80 °C.

Karachi is a humid region in Pakistan. The average value of absolute humidity in May, June and July is 16.3, 17.93 and 20.36 g/kg, respectively. At the same time, the average temperature in Karachi for May, June and July is 34 °C, 35.6 °C and 35.5 °C, respectively. It was found that for moderate and humid climates, the system provides humidity at a comfortable level only when T_{reg} is 80 °C (Figure 14). This means that when the inlet humidity is high, the outlet humidity is also increased and needs a higher regeneration temperature to bring it to a comfortable level. On the other hand, the outlet air temperature is also much affected by higher inlet humidity. The reason is that the efficiency of a direct evaporative cooler is strongly influenced by higher inlet humidity. The outlet temperatures from the system at 60 °C, 70 °C, and 80 °C (T_{reg}) are in the range of 24.9 to 26 °C, 25.5 to 26.9 °C and 26.3 to 27.3 °C, respectively.

The variation in the dehumidification effectiveness of the desiccant wheel for the climatic conditions of three selected cities under different regeneration temperatures is presented in Figure 15. It can be observed that the dehumidification effectiveness shows an increasing trend; this is due to the fact that the specific humidity increases from May to July, and more moisture is available at the inlet of the system. Moreover, it can be clear from the results that the regeneration temperature has significant importance in removing water from the process air. The moisture removal capacity of the desiccant wheel increases with an increase in regeneration temperature. Conversely, a low regeneration temperature of 60 °C results in incomplete moisture removal during regeneration. This will lead to higher residual moisture content in the desiccant wheel, leading to low moisture removal during the dehumidification phase. In regions with high humidity levels (such as the moderate and humid climate of Karachi), the Ed is higher as compared to hot and humid environments or hot and semi-humid climates. This is because the DW can remove maximum moisture from the process air when it contains E_d when regeneration is increased from 60 to 80 °C. The maximum listed E_d at a regeneration temperature of 80 °C for Lahore, Islamabad and Karachi is 0.55, 0.53 and 0.59, respectively.

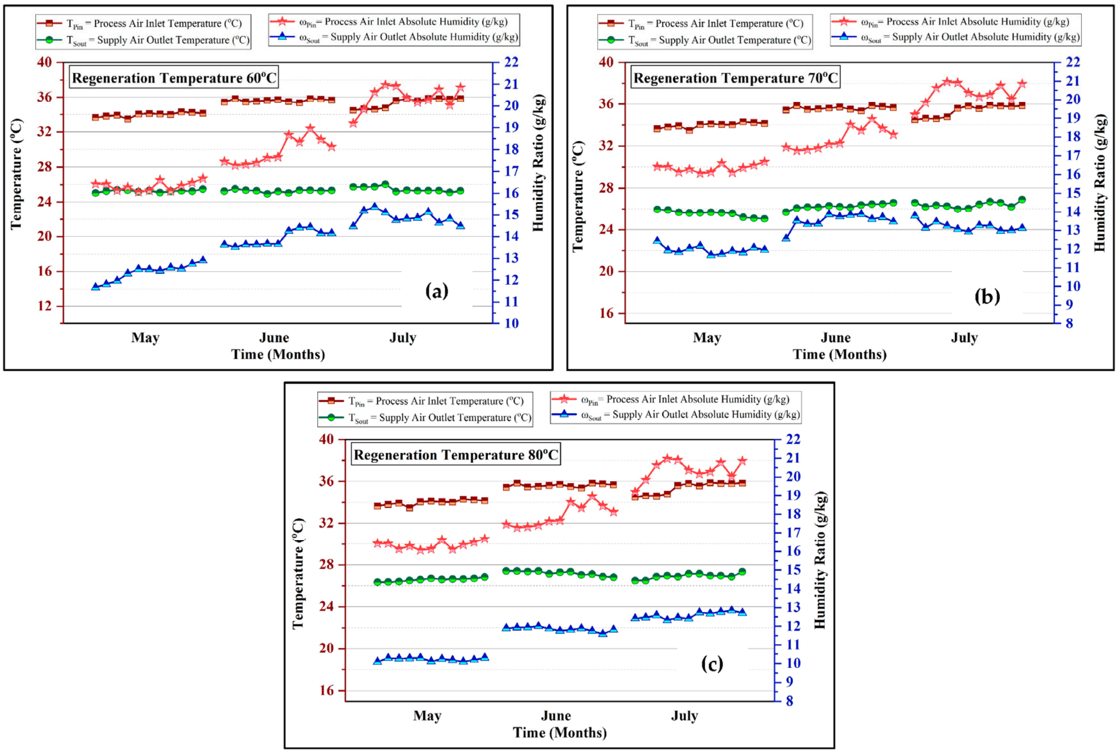

Figure 14. Karachi: variation in temperature and humidity; (**a**) T_{reg} = 60 °C, (**b**) T_{reg} = 70 °C, (**c**) T_{reg} = 80 °C.

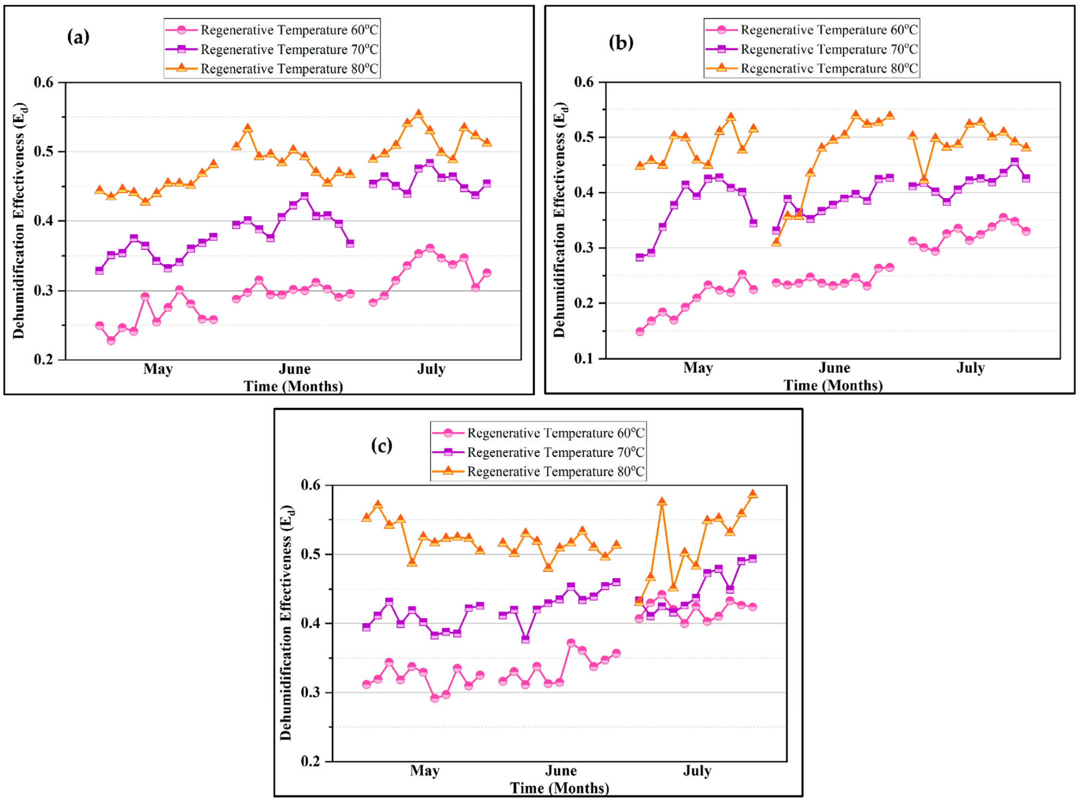

Figure 15. Variation in dehumidification effectiveness: (**a**) Lahore, (**b**) Islamabad, (**c**) Karachi.

The variation in the coefficient of performance of the SDI-DEC for hot and humid, hot and semi-humid, and moderate and humid climates is presented in Figure 16 a–c, respectively. It can be clearly seen that through increasing the regeneration temperature, the COP of the system decreases while, on the other hand, at constant regeneration temperatures such as at 70 °C, the COP shows an increasing trend from May to July. This is because inlet temperature and humidity increase from May to July, resulting in a rise in the COP of the system. Moreover, the results revealed that the COP for the humid climate of the system is lower because at higher inlet humidity, the DW absorbs more moisture. Hence, the system requires more energy to regenerate the desiccant wheel. In a hot and humid climate characterized by high humidity levels and high temperatures (Figure 16a), the COP of the system tends to be the lowest when compared to hot and semi-humid climates (Figure 16b) or moderate and humid climates (Figure 16c). This is primarily due to the fact that an increase in demand for input heat and a higher regeneration temperature is needed in the hot and humid climate as opposed to the conditions in hot and semi-humid climates or moderate and humid climates. The maximum COP achieved at 60 °C (T_{reg}) for Lahore, Islamabad and Karachi is 0.85, 0.87 and 1.06, respectively.

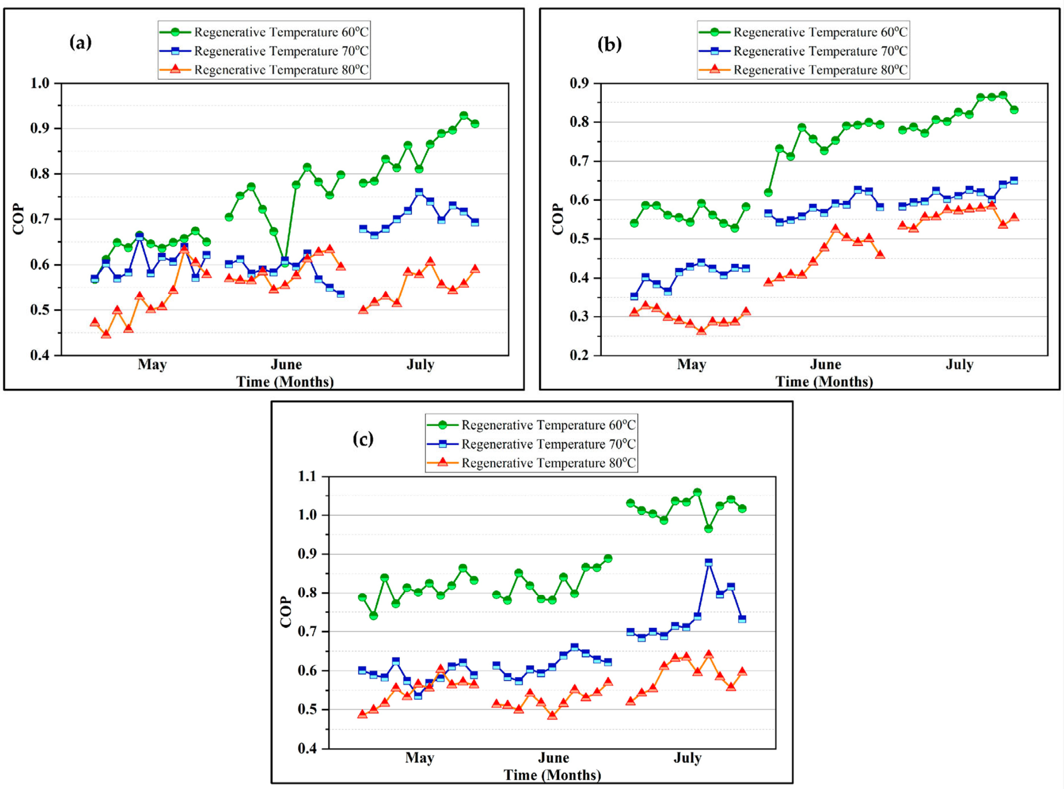

Figure 16. Variation in COP for weather conditions of three cities: (**a**) Lahore, (**b**) Islamabad, (**c**) Karachi.

5. Discussion and Future Work

The use of a specially designed climate chamber to artificially create diverse climatic conditions is a noteworthy aspect of this study. It not only ensures controlled testing but also provides a replicable framework for future research in other geographic regions or for different HVAC technologies and sustainable building technologies worldwide. Due to the availability of controlled environment conditions in the control room, the SDI-DEC system's performance can be assessed for many hot and humid regions like Southeast Asia, Northeast Australia, Africa, and Central and South America. In the future, implementation of the SDI-DEC system can be checked against the requirements of several industries like the agriculture, pharmaceutical, textile and surgical manufacturing sectors, as these industries are facing issues regarding humidity control. Moreover, installed solid desiccant systems can be integrated with various configurations of indirect evaporative coolers under multiple climatic scenarios. In the current study, a silica-gel-based desiccant wheel is used for dehumidification purposes. For further investigation, many other desiccant materials can be tested. Moreover, the SDI-DEC can be tested for year-round application.

6. Conclusions

A solid desiccant integrated with a direct evaporative cooler was designed and developed to analyze the performance of this system under artificially generated climate conditions for the different cities of Lahore, Islamabad and Karachi. This research aimed to test the performance of the SDI-DEC system for the local environmental conditions of Pakistan. Due to high energy costs, the SDI-DEC system has the potential to replace the conventional compression system. Through experimental analysis, it can be concluded that variations in inlet conditions strongly affect the supply air conditions. Under different inlet conditions, the SDI-DEC system is capable of providing supply conditions under thermal comfort levels. The performance of SETCs was also evaluated under different surface areas. Results revealed that the maximum outlet temperature achieved from collectors of a size 9.7 m^2 was 69.1 °C compared to 60 °C from collectors of a size 4.8 m^2. This research will encourage the researcher and users to adopt such technologies, as Pakistan has great potential to harvest solar energy. The current study focuses on the feasibility of the SDI-DEC system under different climate conditions in Pakistan. To serve this purpose, three weather conditions of three different cities of Pakistan were selected. The performance of the system was assessed in terms of COP, E_d and outlet air conditions at regeneration temperatures of 60 °C, 70 °C and 80 °C. The system performs well under comfort levels when the regeneration temperature is set at 70 °C or 80 °C, even with higher inlet humidity.

Furthermore, it was found that in the regions with a high inlet temperature and humidity (e.g., hot and humid), the COP of the system is lower than that in hot and semi-humid climates or moderate and humid climates. Hence, it was concluded that the SDI-DEC system is much more feasible for the hot and semi-humid regions and moderate and humid regions of Pakistan.

Author Contributions: S.U.: Conceptualization, methodology, experimentation, validation, formal analysis, investigation, data curation, writing—original draft, writing—review and editing, and visualization. M.A.: Conceptualization, methodology, validation, investigation, resources, writing—original draft, writing—review and editing, visualization, supervision and project administration. All authors have read and agreed to the published version of the manuscript.

Funding: The authors acknowledge the financial support from the Higher Education Commission (HEC), Pakistan, for this research through the technical development fund (TDF03-337).

Data Availability Statement: Not applicable.

Conflicts of Interest: The authors declare no conflict of interest.

Nomenclature

Abbreviations	Full Form	Symbols	Description
SDI-DEC	Solid desiccant direct evaporative cooler	T_{pin}	Process inlet temperature (°C)
AHU	Air handling unit	T_{sout}	Supply air temperature (°C)
COP	Coefficient of performance	T_{reg}	Regeneration temperature (°C)
DEC	Direct evaporative coolers	E_d	Dehumidification effectiveness
DW	Desiccant wheel	ω_{pin}	Process inlet humidity ratio (g/kg)
HRW	Heat recovery wheel	ω_{sout}	Specific humidity of supply air (g/kg)
IDEC	Indirect evaporative coolers	h	Enthalpy of air (kJ/kg)
SETCs	Solar evacuated tube collectors	$\dot{m}$	Mass flow rate of water (kg/s)
SF	Solar fraction	Q_{gain}	Useful energy gain (kW)
M-Cycle	Maisotsenko cycle	Q_{sol}	Solar Energy W/m^2
		c_p	Specific heat (J/kgK)

References

1. Rahman, A.; Abas, N.; Dilshad, S.; Shoaib, M. Case Studies in Thermal Engineering A case study of thermal analysis of a solar assisted absorption air-conditioning system using R-410A for domestic applications. *Case Stud. Therm. Eng.* **2021**, *26*, 101008. [CrossRef]
2. De Almeida, C.R.; Albuquerque Neto, C.; Tsuha, C.d.H.C.; Boscov, M.E.G. Numerical study on heat transfer performance of geothermal piles in a Brazilian sandy soil. *Soils Rocks* **2022**, *45*, e2022076621. [CrossRef]
3. Wrobel, J.; Morgenstern, P.; Schmitz, G. Modeling and experimental validation of the desiccant wheel in a hybrid desiccant air conditioning system. *Appl. Therm. Eng.* **2013**, *51*, 1082–1091. [CrossRef]
4. Habib, M.F.; Ali, M.; Sheikh, N.A.; Badar, A.W.; Mehmood, S. Building thermal load management through integration of solar assisted absorption and desiccant air conditioning systems: A model-based simulation-optimization approach. *J. Build. Eng.* **2020**, *30*, 101279. [CrossRef]
5. Ghenai, C.; Salameh, T. *Sustainable Air Conditioning Systems*; BoD–Books on Demand: Norderstedt, Germany, 2018; ISBN 1789233003.
6. Cuce, E.; Sher, F.; Sadiq, H.; Cuce, P.M.; Guclu, T.; Besir, A.B. Sustainable ventilation strategies in buildings: CFD research. *Sustain. Energy Technol. Assess.* **2019**, *36*, 100540. [CrossRef]
7. Rafique, M.M.; Gandhidasan, P.; Rehman, S.; Al-Hadhrami, L.M. A review on desiccant based evaporative cooling systems. *Renew. Sustain. Energy Rev.* **2015**, *45*, 145–159. [CrossRef]
8. Libra, M.; Mrázek, D.; Tyukhov, I.; Severová, L.; Poulek, V.; Mach, J.; Šubrt, T.; Beránek, V.; Svoboda, R.; Sedláček, J. Reduced real lifetime of PV panels–Economic consequences. *Sol. Energy* **2023**, *259*, 229–234. [CrossRef]
9. Kumar, K.; Singh, A.; Chaurasiya, P.K.; Pathak, K.K.; Pandey, V. Progressive development in hybrid liquid desiccant-vapour compression cooling system: A review. *Sustain. Energy Technol. Assess.* **2023**, *55*, 102960. [CrossRef]
10. Ditta, A.; Tabish, A.N.; Mujtaba, M.A.; Chaudhary, G.Q.; Razzaq, L. Experimental investigation of a hybrid con fi guration of solar thermal collectors and desiccant indirect evaporative cooling system. *Front. Energy Res.* **2022**, *10*, 979942. [CrossRef]
11. Misha, S.; Mat, S.; Ruslan, M.H.; Sopian, K. Review of solid/liquid desiccant in the drying applications and its regeneration methods. *Renew. Sustain. Energy Rev.* **2012**, *16*, 4686–4707. [CrossRef]
12. Luo, J.; Yang, H. A state-of-the-art review on the liquid properties regarding energy and environmental performance in liquid desiccant air-conditioning systems. *Appl. Energy* **2022**, *325*, 119853. [CrossRef]
13. Motaghian, S.; Pasdarshahri, H. Regeneration energy analysis and optimization in desiccant wheels using purge mechanism. *J. Build. Eng.* **2020**, *27*, 100980. [CrossRef]
14. Wu, X.N.; Ge, T.S.; Dai, Y.J.; Wang, R.Z. Investigation on novel desiccant wheel using wood pulp fiber paper with high coating ratio as matrix. *Energy* **2019**, *176*, 493–504. [CrossRef]
15. Fu, H.-X.; Zhang, L.-Z.; Xu, J.-C.; Cai, R.-R. A dual-scale analysis of a desiccant wheel with a novel organic–inorganic hybrid adsorbent for energy recovery. *Appl. Energy* **2016**, *163*, 167–179. [CrossRef]
16. Asim, N.; Amin, M.H.; Alghoul, M.A.; Badiei, M.; Mohammad, M.; Gasaymeh, S.S.; Amin, N.; Sopian, K. Key factors of desiccant-based cooling systems: Materials. *Appl. Therm. Eng.* **2019**, *159*, 113946. [CrossRef]
17. Chen, C.-H.; Hsu, C.-Y.; Chen, C.-C.; Chen, S.-L. Silica gel polymer composite desiccants for air conditioning systems. *Energy Build.* **2015**, *101*, 122–132. [CrossRef]
18. Daneshazarian, R.; Cuce, E.; Cuce, P.M.; Sher, F. Concentrating photovoltaic thermal (CPVT) collectors and systems: Theory, performance assessment and applications. *Renew. Sustain. Energy Rev.* **2018**, *81*, 473–492. [CrossRef]
19. Ali, M.; Vukovic, V.; Muhammad Ali, H.; Ahmed Sheikh, N. Performance analysis of solar-assisted desiccant cooling system cycles in world climate zones. *J. Sol. Energy Eng.* **2018**, *140*, 41009. [CrossRef]
20. Rafique, M.M.; Rehman, S.; Lashin, A.; Al Arifi, N. Analysis of a solar cooling system for climatic conditions of five different cities of Saudi Arabia. *Energies* **2016**, *9*, 75. [CrossRef]
21. Jani, D.B.; Mishra, M.; Sahoo, P.K. Performance analysis of a solid desiccant assisted hybrid space cooling system using TRNSYS. *J. Build. Eng.* **2018**, *19*, 26–35. [CrossRef]
22. Gao, W.; Worek, W.; Konduru, V.; Adensin, K. Numerical study on performance of a desiccant cooling system with indirect evaporative cooler. *Energy Build.* **2015**, *86*, 16–24. [CrossRef]
23. Fong, K.F.; Chow, T.T.; Lee, C.K.; Lin, Z.; Chan, L.S. Advancement of solar desiccant cooling system for building use in subtropical Hong Kong. *Energy Build.* **2010**, *42*, 2386–2399. [CrossRef]
24. Ali, M.; Vukovic, V.; Ahmed, N.; Ali, H.M. Performance investigation of solid desiccant evaporative cooling system configurations in different climatic zones. *Energy Convers. Manag.* **2015**, *97*, 323–339. [CrossRef]
25. Belguith, S.; Meddeb, Z.; Ben Slama, R. Performance analysis of desiccant cooling systems in a hot and dry climate. *Euro-Mediterr. J. Environ. Integr.* **2021**, *6*, 1–11. [CrossRef]
26. Lai, L.; Wang, X.; Kefayati, G.; Hu, E. Evaporative Cooling Integrated with Solid Desiccant Systems: A Review. *Energies* **2021**, *14*, 5982. [CrossRef]
27. Rafique, M.M.; Gandhidasan, P.; Rehman, S.; Alhems, L.M. Performance analysis of a desiccant evaporative cooling system under hot and humid conditions. *Environ. Prog. Sustain. Energy* **2016**, *35*, 1476–1484. [CrossRef]
28. Joudi, K.A.; Dhaidan, N.S. Application of solar assisted heating and desiccant cooling systems for a domestic building. *Energy Convers. Manag.* **2001**, *42*, 995–1022. [CrossRef]

29. Hindoliya, D.A.; Mullick, S.C. Assessment of utilisation potential of direct evaporative cooling for India. *Int. J. Ambient Energy* **2006**, *27*, 21–28. [CrossRef]
30. Bourdoukan, P.; Wurtz, E.; Joubert, P. Experimental investigation of a solar desiccant cooling installation. *Sol. Energy* **2009**, *83*, 2059–2073. [CrossRef]
31. Heidarinejad, G.; Pasdarshahri, H. Potential of a desiccant-evaporative cooling system performance in a multi-climate country. *Int. J. Refrig.* **2011**, *34*, 1251–1261. [CrossRef]
32. Delfani, S.; Karami, M. Transient simulation of solar desiccant/M-Cycle cooling systems in three different climatic conditions. *J. Build. Eng.* **2020**, *29*, 101152. [CrossRef]
33. Parmar, H.; Hindoliya, D.A. Performance of solid desiccant-based evaporative cooling system under the climatic zones of India. *Int. J. Low-Carbon Technol.* **2013**, *8*, 52–57. [CrossRef]
34. El, M.; Ghaddar, N.; Ghali, K.; Itani, M. Hybrid cooling system integrating PCM-desiccant dehumidification and personal evaporative cooling for hot and humid climates. *J. Build. Eng.* **2021**, *33*, 101580. [CrossRef]
35. Khosravi, N.; Aydin, D.; Karim, M.; Abohorlu, P. Comparative performance analysis of direct and desiccant assisted evaporative cooling systems using novel candidate materials. *Energy Convers. Manag.* **2020**, *221*, 113167. [CrossRef]
36. Lee, Y.; Park, S.; Kang, S. Performance analysis of a solid desiccant cooling system for a residential air conditioning system. *Appl. Therm. Eng.* **2020**, *182*, 116091. [CrossRef]
37. Song, J.; Sobhani, B. Energy and exergy performance of an integrated desiccant cooling system with photovoltaic/thermal using phase change material and maisotsenko cooler. *J. Energy Storage* **2020**, *32*, 101698. [CrossRef]
38. Samad, A.; Waheed, A.; Bilal, M.; Fatima, M.; Zahra, A.; Siddiqui, M.S. Dynamic simulation and parametric analysis of solar assisted desiccant cooling system with three configuration schemes. *Sol. Energy* **2020**, *197*, 22–37. [CrossRef]
39. Berardi, U.; Heidarinejad, G.; Rayegan, S.; Pasdarshahri, H. Enhancing the cooling potential of a solar-assisted desiccant cooling system by ground source free cooling. In *Building Simulation*; Tsinghua University Press: Beijing, China, 2020; pp. 1125–1144.
40. Ahmad, W.; Ali, M.; Sheikh, N.A. Effect of efficient multi-stage indirect evaporative cooling on performance of solar assisted desiccant air conditioning in different climatic zones. *Heat Mass Transf.* **2020**, *56*, 2725–2741. [CrossRef]
41. Karami, M.; Delfani, S.; Noroozi, A. Performance characteristics of a solar desiccant/M-cycle air-conditioning system for the buildings in hot and humid areas. *Asian J. Civ. Eng.* **2020**, *21*, 189–199. [CrossRef]
42. Weather Atlas, Pakistan. Detailed Climate Information and Monthly Weather Forecast. 2023. Available online: https://www.weather-atlas.com/en/pakistan/climate (accessed on 15 April 2023).